Nanotechnology **21** (2010) 455201 (5pp) doi:10.1088/0957-4484/21/45/455201

Electroluminescence from silicon nanoparticles fabricated from the gas phase

Jens Theis[1], Martin Geller[1], Axel Lorke[1], Hartmut Wiggers[2], Andreas Wieck[3] and Cedrik Meier[4]

[1] Fakultät für Physik and CeNIDE, Universität Duisburg-Essen, D-47048 Duisburg, Germany
[2] Institut für Verbrennung und Gasdynamik and CeNIDE, Universität Duisburg-Essen, D-47048 Duisburg, Germany
[3] Angewandte Festkörperphysik, Ruhr-Universität Bochum, D-44780 Bochum, Germany
[4] Experimental Physics and CeOPP, Universität Paderborn, D-33098 Paderborn, Germany

Received 30 June 2010, in final form 22 September 2010
Published 14 October 2010
Online at stacks.iop.org/Nano/21/455201

Abstract
Electroluminescence from as-prepared silicon nanoparticles, fabricated by gas phase synthesis, is demonstrated. The particles are embedded between an n-doped GaAs substrate and a semitransparent indium tin oxide top electrode. The total electroluminescence intensity of the Si nanoparticles is more than a factor of three higher than the corresponding signal from the epitaxial III–V semiconductor. This, together with the low threshold voltage for electroluminescence, shows the good optical properties of these untreated particles and the efficient electrical injection into the device. Impact ionization by electrons emitted from the top electrode is identified as the origin of the electrically driven light emission.

(Some figures in this article are in colour only in the electronic version)

The discovery of room-temperature photoluminescence (PL) from porous silicon in 1990 [1] resulted in an increasing interest in the optical properties of nanoscopic silicon and particularly in the possibility of fabricating electroluminescence (EL) devices. A number of groups have investigated the EL properties of silicon nanocrystals, embedded in a silicon dioxide matrix [2–7]. These nanocrystals can be produced, e.g., using substoichiometric silicon oxide or by silicon ion implantation in silicon dioxide and subsequent annealing. So far, little work is available on EL from nanoparticle powders [5]. Such powders may be of great interest for cost effective production of Si-based optoelectronics because they can be used in low-temperature processes for printed electronics on transparent, flexible substrates, such as polymers. In this respect, silicon nanoparticles (Si-NPs) are similar to organic semiconductors but, additionally, they are based on stable, low-cost, non-toxic material. Furthermore, the synthesis is scalable up to the kg scale. Here, we present an EL device, which is based on untreated Si-NPs from the gas phase. The particle layer in the optically active (light emitting) region is fabricated using a simple drop-casting technique. Spectrally resolved EL studies show an efficient light emission from the particles, which is induced by electrons and holes generated by impact ionization.

The Si-NPs used in this work were produced from the gas phase in a low pressure microwave reactor using silane (SiH_4) as precursor. These particles show a lognormal size distribution with a mean diameter of 3.9 nm. They consist of a single-crystalline silicon core and—after storage under ambient conditions—a 1–2 nm thick, amorphous silicon dioxide shell. A high-resolution TEM image of this type of particles can be found in an article by Gupta *et al* [8]. The mean diameter of the nanoparticles was estimated from the wavelength of the PL maximum and using the equation described by Ledoux *et al* [9]. Further details of the nanoparticle synthesis and particle formation can be found in [10, 11]; their optical properties have been investigated in [12–15].

The schematic steps of sample preparation and a cross-section of the sample design can be seen in figures 1(a) and (b), respectively. As substrate material, we use a GaAs heterostructure. It consists of a 300 nm n-conducting (Si-doped) GaAs layer and a 100 nm thick intrinsic GaAs layer, grown on semi-insulating GaAs by molecular-beam-epitaxy.

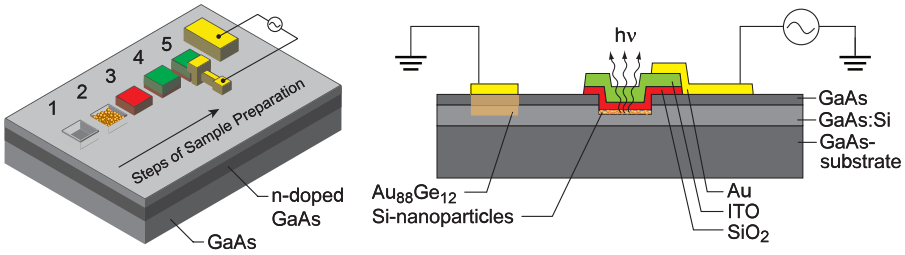

Figure 1. (a) Schematic picture of the steps of sample preparation. From left to right: 1 etching, 2 Si-NP deposition, 3 SiO_2 (red) evaporation and lift-off, 4 indium tin oxide (green) deposition, and 5 evaporation of metallic top contacts. (b) A schematic cross-section of the EL device, with the optically active Si-NP layer sandwiched between the highly doped GaAs substrate and a transparent indium tin oxide top electrode.

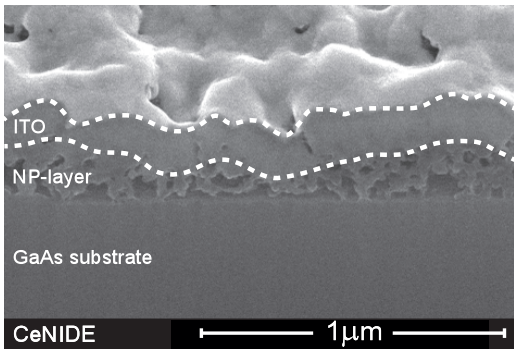

Figure 2. Cross-section scanning electron microscope (SEM) image (angle of view is 45°) of the EL device. A focused ion beam (FIB) was used to create a cross-sectional cut into the surface of the device.

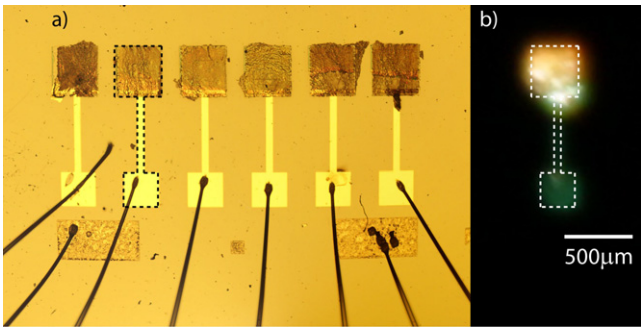

Figure 3. (a) Picture of the processed wafer with six Si-NP devices. All six devices are operable as active light emitters. (b) Picture of the second device under operating conditions. The light emission can be seen with the unaided eye. The orange light originates from the embedded nanoparticles, whereas the green light at the gold contacts is attributed to Au surface plasmons.

Using photolithographic masking, recess areas are etched (H_2SO_4-based etchant) through the insulating GaAs layer into the conducting layer (step 1 in figure 1(a)). A small amount of the nanoparticle powder is dispersed in a solution of distilled water and 5% ethanol, using 15 min ultrasonic agitation. The dispersion is drop-cast onto the sample and the solvent is given time to evaporate (step 2). On top of the nanoparticle film, a 10 nm thick SiO_2 protection layer (step 3) and a 80 nm thick indium tin oxide (ITO) layer (step 4) are evaporated via e-beam evaporation. After the photoresist lift-off, which removes all material outside the recess areas, the sample is annealed for 30 min at 380 °C in the presence of oxygen to transform the as-deposited ITO layer into a conductive transparent film. Electrical contact to the buried n-doped GaAs layer is obtained by the diffusion of an $Au_{88}Ge_{12}$ alloy. In the final processing step, 50 nm thick Au contacts are defined by a second photolithographic lift-off step (step 5). The final device is shown in cross-section in figure 2. The nanoparticle layer has an average thickness of 150 nm with large variations and local film thicknesses of up to 500 nm. For comparison, a reference sample was fabricated using identical processing steps, but without deposition of the Si-NPs. Furthermore, a sample with a layer of Si-NPs from the same batch as those used in the device was prepared on an undoped silicon substrate.

For the present 'proof-of-concept'-study, a GaAs heterostructure was used as a substrate, which has two advantages: first, conducting and (semi-) insulating layers can be fabricated and patterned with high accuracy. Second, the high index of refraction, together with the smooth etched surface, make this substrate highly reflecting for the light emitted from the particles. On the other hand, the disadvantage of using GaAs is that this material itself exhibits luminescence at a wavelength of 870 nm as a result of its direct bandgap of 1.42 eV.

Figure 3(a) shows a picture of the processed sample with six EL devices mounted on a chip carrier and wire bonded. Clearly visible at the top of the picture are the square active regions with the drop-cast nanoparticle layer. All six devices are operable. Figure 3(b) shows the second device under operating conditions with a dc voltage of 5.6 V and a current of 51 mA. The EL in the visible spectral range can be seen with the unaided eye. In figure 3(b) a photographic image of one active EL device is shown taken with a commercial DSLR camera (Canon EOS 400D using an exposure time of 15 s at ISO 200 and F5.6). The orange light originates from the embedded nanoparticles in the EL device. We attribute the faint green luminescence at the gold contacts below the active layer to Au surface plasmons.

To spectrally resolve the contribution to the bright luminescence from the nanoparticles and GaAs substrate, EL and PL measurements were conducted in a PL setup using a frequency doubled Nd:YAG laser (wavelength 532 nm) for excitation and a CCD as a detector. The sample was first electrically excited by a square wave signal with a frequency of 10 kHz, a maximum amplitude of 5 V (corresponding to a peak-to-peak amplitude of 10 V) and no DC bias offset.

In figure 4(a), the light intensity as a function of the emission wavelength is shown for different AC voltages V_{AC}.

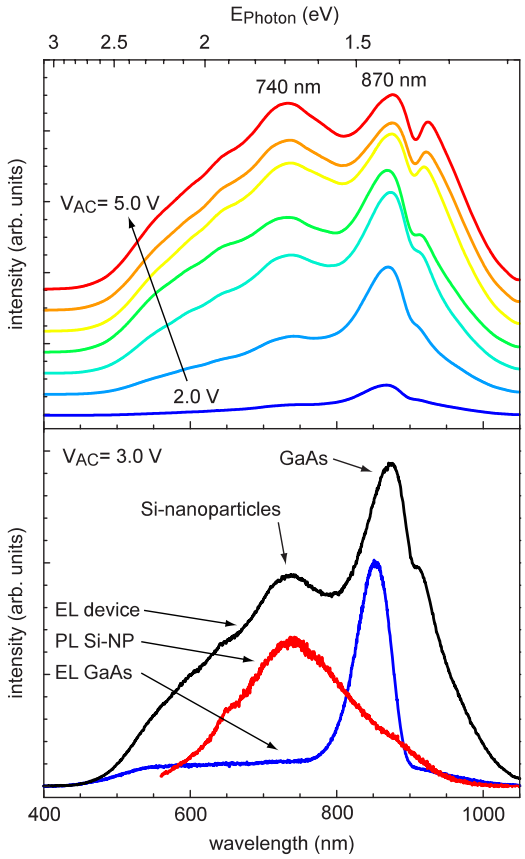

Figure 4. (a) EL emission spectra at different AC voltages ranging from 2.0 to 5.0 V in steps of 0.5 V. (b) Comparison between the EL of the device (black) at 3.0 V with the EL of a reference sample without Si-NPs (blue) and the photoluminescence of Si-NPs (red) on a silicon substrate.

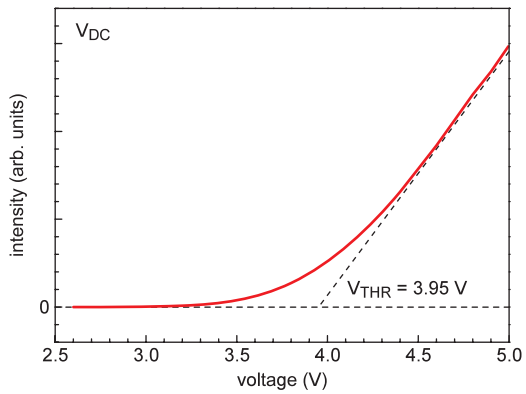

Figure 5. The Intensity of the EL emission from the Si-NPs at 740 nm as a function of the applied DC voltage at the top electrode.

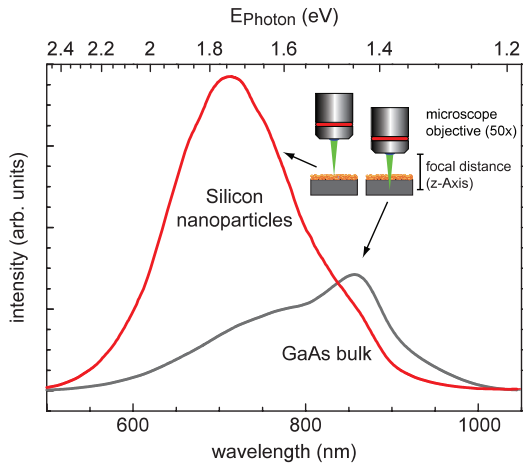

Figure 6. Spectra of the EL emission from the device. The focal point of the microscope objective was set to the silicon nanoparticle layer (red curve) or the GaAs bulk material (gray curve), respectively. The integrated emission intensity from the Si-NP layer is more than three times higher than that from the GaAs substrate.

At $V_{AC} \leqslant 1.7$ V, no light emission from the device is detectable. For $V_{AC} \geqslant 2.0$ V, we observe a pronounced peak around 870 nm (1.42 eV) and a broad contribution around 740 nm (1.68 eV). With increasing voltage, the 740 nm peak reaches almost the same intensity as the 870 nm emission. Another small peak develops around 920 nm (1.35 eV) at $V_{AC} > 4.0$ V.

In figure 4(b), the EL emission from the device at 3.0 V is compared with the PL spectrum of the Si-NPs. It can be seen that the PL maximum at 740 nm exactly matches the peak in the EL of our device. Furthermore, the EL maximum at 870 nm from the reference sample without Si-NPs matches the second peak of the EL device. In fact, it is possible to reproduce the EL in figure 4(b) by appropriate superposition of the spectral characteristics of the two reference samples [16]. From these findings we conclude that the observed EL emission at 740 nm originates from the Si-NPs, while the line at 870 nm is caused by emission from the GaAs substrate [17]. The additional peak at 920 nm can be attributed to sub-bandgap luminescence caused by donor states in the Si-doped GaAs layer.

A measurement of the light emission intensity as a function of the applied dc voltage at the top electrode is shown in figure 5. For a low voltage no light emission is observed, which changes from an exponential to a linear behavior for a driving voltage of more than 4.5 V.

In order to demonstrate the light generation of the Si-NPs (even in the presence of an optical active GaAs substrate), we measured the EL in a micro-PL setup with a 50-fold magnification in confocal geometry. This enables us to shift the focus into the nanoparticle layer and the GaAs bulk material separately, in order to compare the efficiency of the light generation in the silicon nanoparticles with the direct bandgap material GaAs (see inset in figure 6). The red curve in figure 6 shows the EL spectrum with the focus within the silicon nanoparticle layer. The spectrum is dominated by the nanoparticle luminescence with a maximum centered at 740 nm and a full width at half maximum of about 150 nm. The GaAs contribution is only seen as a very weak shoulder at 850 nm. Setting the focus into the GaAs substrate reduces the Si-NP contribution significantly while the GaAs luminescence is increased, cf gray curve in figure 6. Comparing the spectrum from the Si-NPs (red curve) with the GaAs bulk spectrum (gray curve) in figure 6 suggests that the Si-NPs are efficient light emitters in such EL devices, since the integrated emission intensity from the nanoparticle layer is more than three times higher than that from the GaAs substrate.

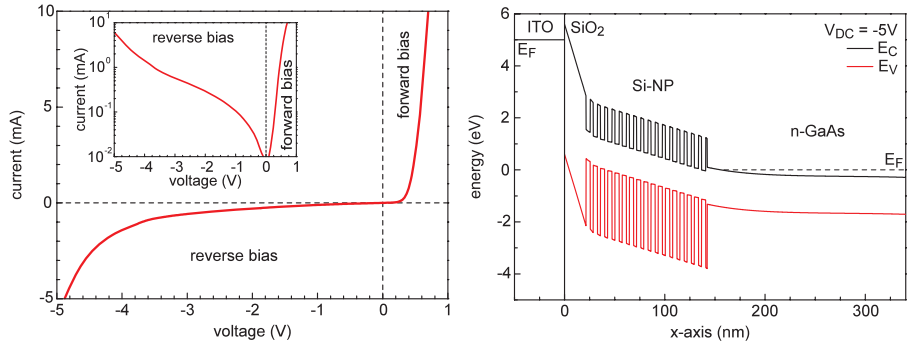

Figure 7. (a) Measured IV-curve of an EL device. The inset shows the same IV-curve but on a logarithmic scale. (b) Calculated one-dimensional band structure of the EL device by solving the Poisson equation. The quantum wells visible in the band structure represent the Si/SiO_2 core/shell nanoparticles.

An important question relates to the origin of the observed EL. In the literature, mainly two different mechanisms have been proposed: on the one hand, injection of electrons and holes from either different electrodes [5, 7] or a single electrode [4], on the other hand, electron–hole pair generation by impact ionization [2, 3, 18].

To better understand the origin of the visible luminescence in the present device, we have also investigated its DC bias response without AC modulation. We find that the current–voltage (I–V) characteristic shown in figure 7(a) exhibits a diode-like behavior with the high resistance state for negative bias applied to the top electrode. The inset in figure 7(a) shows the I–V curve on a semilogarithmic plot. The measured IV-characteristic of the device under forward bias can be well described using the common (Shockley-type) formula for a metal–semiconductor contact with a Schottky barrier of $V_{\text{Schottky}} = 0.6$ V. This is in good agreement with the measured onset voltage in forward bias, $V_{\text{onset}} = 0.5$ V. Most likely, because of the roughness of the nanoparticle layer, the deposited SiO_2 layer is not continuous, so that in some parts of the sample, the metallic ITO is in direct contact with the Si nanoparticles.

No EL is observed for positive bias. For negative DC voltages, EL of similar or higher brightness than for AC driving is emitted. This excludes a mechanism such as the one discussed by Walters *et al* [4] as an explanation for the light emission of the present device.

Further conclusions can be drawn from the fact that EL emission is only observed for negative bias at the top electrode. A simulation of the band structure of the device using a 1D Poisson equation solver [19] is shown in figure 7(b). The simulation shows that under bias conditions, which lead to EL, no holes can be injected from the n-doped GaAs substrate. Also, the quasi-metallic top electrode will only emit electrons under negative bias. The lack of hole injection from either top or bottom electrode leads us to conclude that the observed EL emission is driven by impact ionization, caused by electrons accelerated from the top electrode towards the back contact. The electron–hole pairs, induced by scattering of highly excited electrons, recombine radiatively in the Si-NPs.

In closing, we would like to mention that the onset of the EL shows a clear threshold at 4.0 V, considerably less than what has been reported in other studies. It should also be pointed out that the nanoparticles are 'as synthesized', i.e., no etching, functionalization or other treatment was employed. No high-temperature step is necessary for the Si-NP layer fabrication, which promises the use of polymer-based, flexible foils as substrates for these devices. Furthermore, the evaporated ITO layer can in principle be replaced by a layer of ITO particles [20], which are commercially available today. Finally, the lift-off processes can be replaced by ink-jet printing [21]. This suggests that untreated Si-NPs from the gas phase are an excellent starting material for fabricating efficient, low-cost, non-toxic light emitters.

Acknowledgments

Financial support by the DFG through the grants GRK 1240 and SFB445 as well as support by BMBF through the Nanofutur program (grant 03X5509) is gratefully acknowledged.

References

[1] Canham L T 1990 *Appl. Phys. Lett.* **57** 1046
[2] Irrera A, Pacifici D, Miritello M, Franzo G and Priolo F 2002 *Appl. Phys. Lett.* **81** 1866
[3] Valenta J, Lalic N and Linnros J 2004 *Appl. Phys. Lett.* **84** 1459
[4] Walters R J, Borianoff G I and Atwater H A 2005 *Nat. Mater.* **4** 143
[5] Fojtik A, Valenta J, Stuchlikova T H, Stuchlik J, Pelant I and Kocka J 2006 *Thin Solid Films* **515** 775
[6] Carreras J, Arbiol J, Garrido B, Bonafos C and Montserrat J 2008 *Appl. Phys. Lett.* **92** 091103
[7] Xu J, Makihara K, Deki H and Miyazaki S 2009 *Solid State Commun.* **149** 739
[8] Gupta A, Swihart M T and Wiggers H 2009 *Adv. Funct. Mater.* **19** 696
[9] Ledoux G, Guillois O, Porterat D, Reynaud C, Huisken F, Kohn B and Paillard V 2000 *Phys. Rev.* B **62** 15942
[10] Knipping J, Wiggers H, Rellinghaus B, Roth P, Konjhodzic D and Meier C 2004 *J. Nanosci. Nanotechnol.* **4** 1039

[11] Giesen B, Wiggers H, Kowalik A and Roth P 2005 *J. Nanopart. Res.* **7** 29
[12] Kravets V G, Meier C, Konjhodzic D, Lorke A and Wiggers H 2005 *J. Appl. Phys.* **97** 084306
[13] Meier C, Lüttjohann S, Kravets V G, Nienhaus H, Lorke A and Wiggers H 2006 *Physica* E **32** 155
[14] Lüttjohann S, Meier C, Offer M, Lorke A and Wiggers H 2007 *Europhys. Lett.* **79** 37002
[15] Meier C, Gondorf A, Lüttjohann S and Lorke A 2007 *J. Appl. Phys.* **101** 103112
[16] Theis J 2009 *Diploma Thesis* Univerity of Duisburg-Essen
[17] Madelung O, Rössler U and Schulz M (ed) *Gallium Arsenide (GaAs), Exciton Ground and Excited States* (*Springer Materials—The Landolt-Börnstein Database*) doi:10.1007/10832182_174
[18] Liu C W, Chang S T, Liu W T, Chen M-J and Lin C-F 2000 *Appl. Phys. Lett.* **77** 4347
[19] Tan I-H, Snider G L and Hu E L 1990 *J. Appl. Phys.* **68** 4071
[20] Prodi-Schwab A, Lüthge T, Jahn R, Herbig B and Löbmann P 2008 *J. Sol–Gel Sci. Technol.* **47** 68
[21] Gupta A, Khalil A S G, Offer M, Geller M, Winterer M, Lorke A and Wiggers H, unpublished